Supplementary information

Thin films composed of Zr-doped In_2O_3 grains rich in fracture surfaces and cracks for photoelectrochemical water oxidation

Shu Yang,[a] Changlong Chen,*[a] Yuling Wei,[b] Leshuang Wang,[a] Qiang Liu,[a] Liya Jiang[a] and Guobao Li[a]

[a] *School of Chemistry and Chemical Engineering, University of Jinan, Jinan, 250022, Shandong, China*
[b] *State Key Laboratory of Biobased Material and Green Papermaking, Qilu University of Technology (Shandong Academy of Sciences), Jinan 250353, Shandong, China*

*Corresponding author.
E-mail address: chm_chencl@ujn.edu.cn (C. Chen)

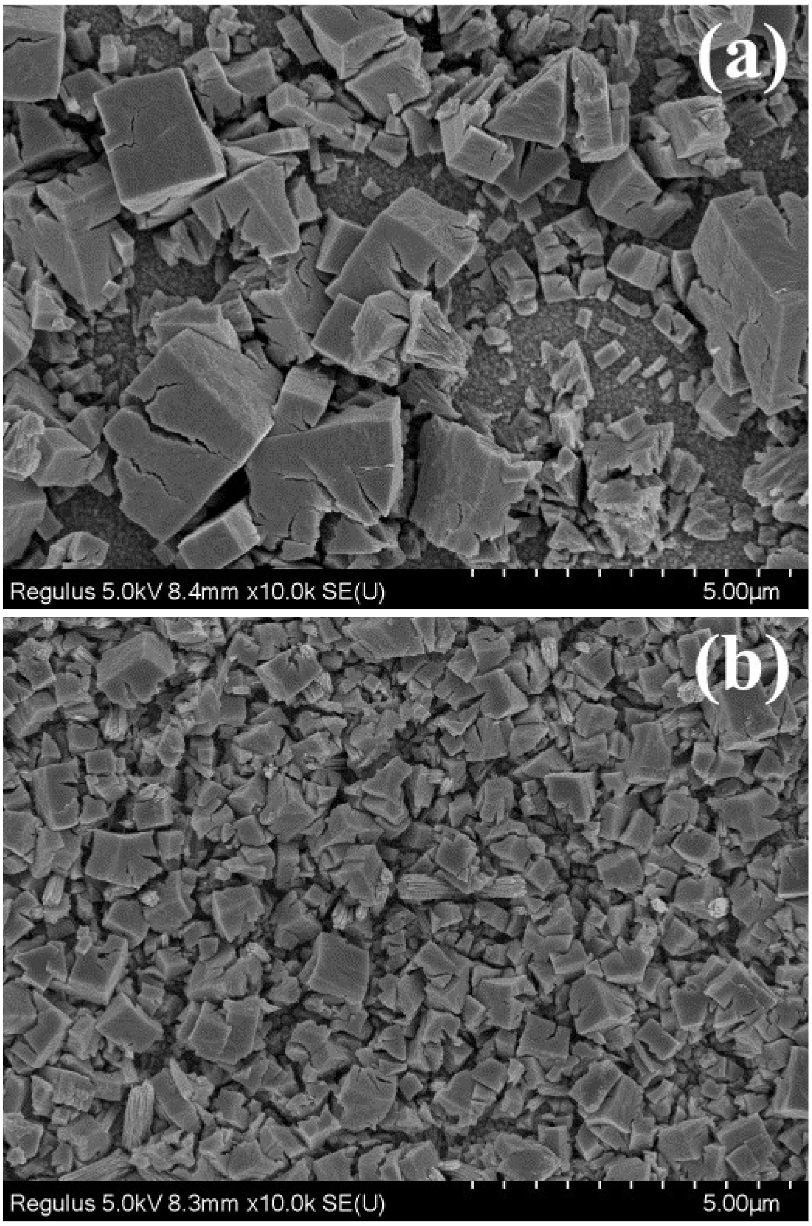

Fig. S1 SEM images of undoped In_2O_3 (a) and 14.5%-Zr-In_2O_3 (b) samples.

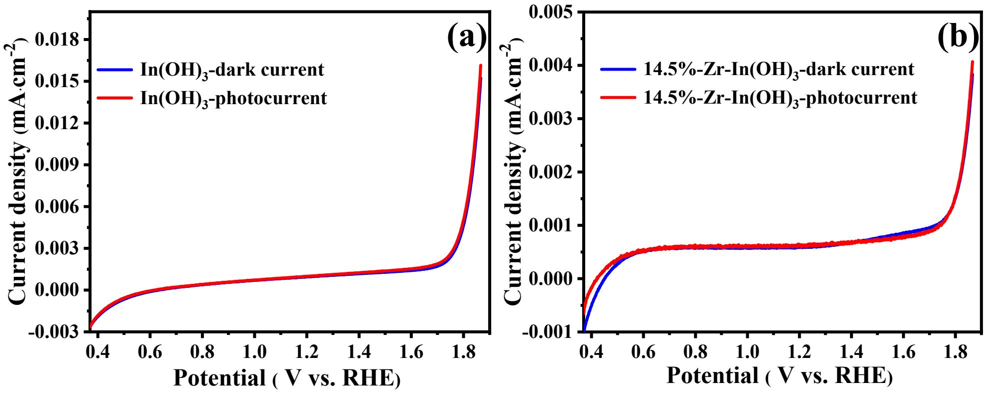

Fig. S2 LSV curves of the undpoed and 14.5%-Zr-$In(OH)_3$ films measured under AM1.5G illumination at 100 mW·cm^{-2} and in dark.

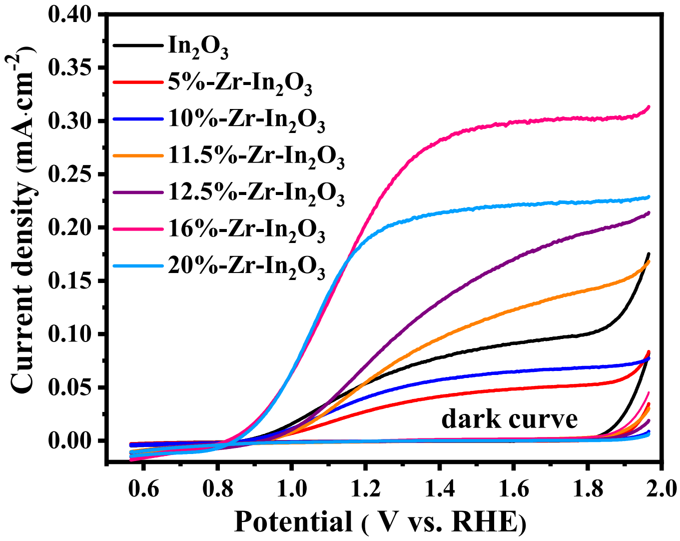

Fig. S3 LSV curves of undpoed and Zr-doped In_2O_3 films measured under AM1.5G illumination at 100 mW·cm^{-2} and in dark.

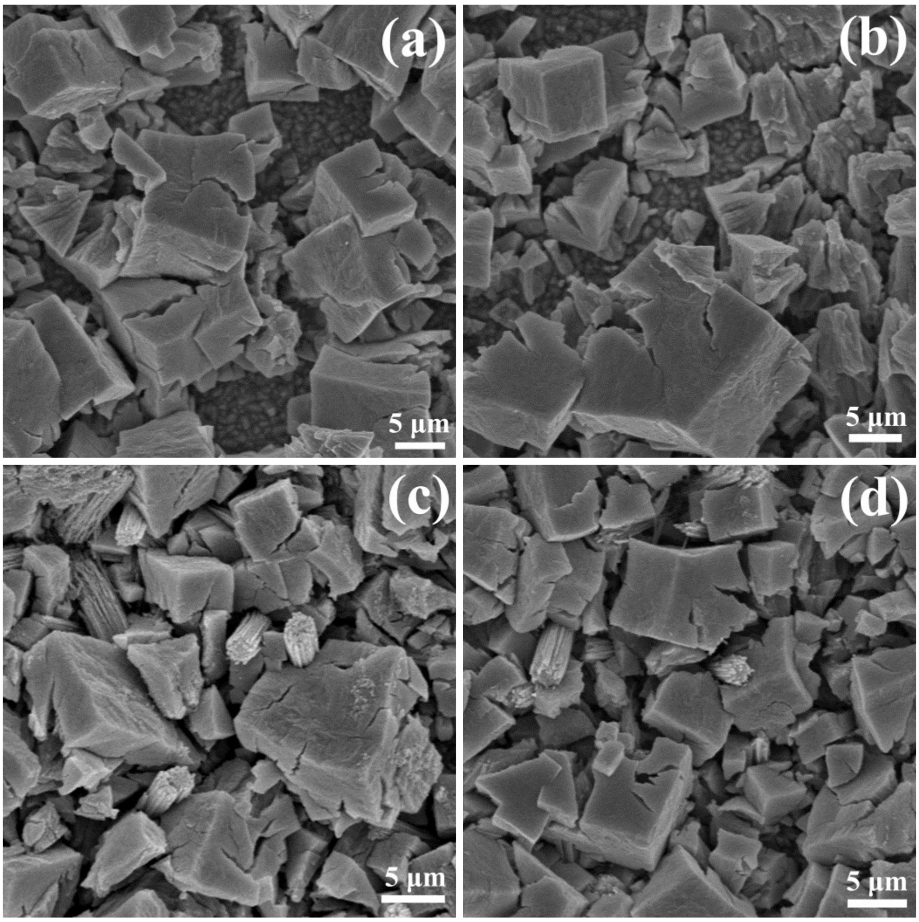

Fig. S4 SEM images of In_2O_3 before (a) and after (b) PEC test; SEM images of 14.5%-Zr-In_2O_3 before (c) and after (d) PEC test.

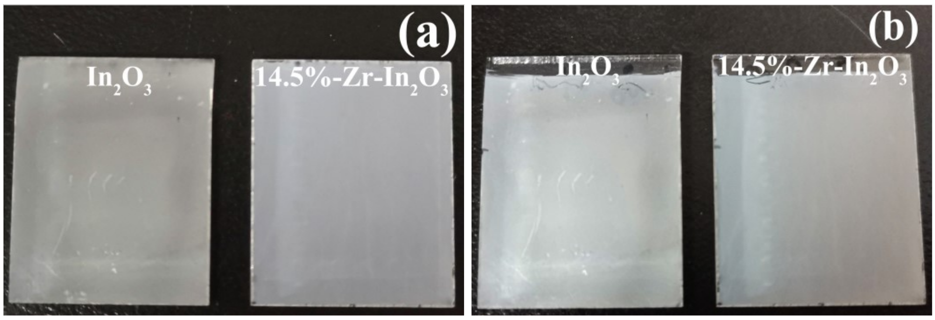

Fig. S5 The optical photos of In_2O_3 and 14.5%-Zr-In_2O_3 samples before (a) and after (b) PEC tests.

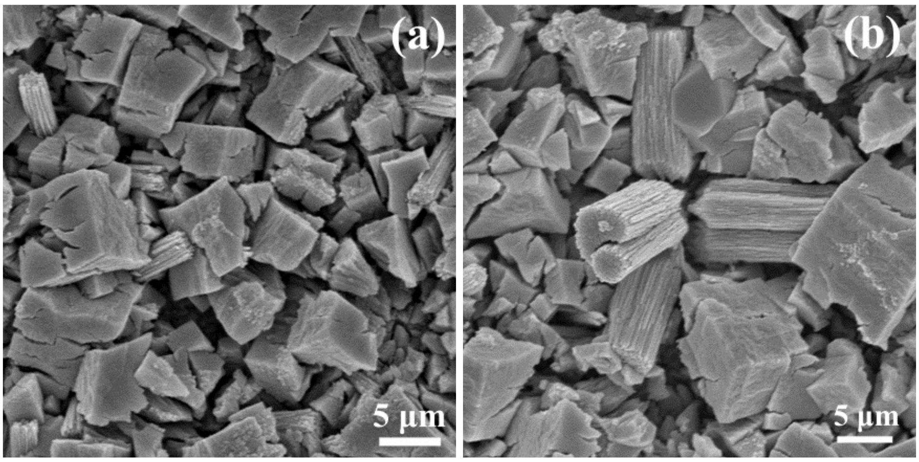

Fig. S6 SEM images of 14.5%-Zr-In_2O_3 prepared from 14.5%-Zr-$In(OH)_3$ with a heating rate of (a) 0.5°C·min^{-1} and (b) 3°C·min^{-1}.

Table S1 The contents of In, O and Zr in the Zr-doped In_2O_3 samples measured by EDS.

Sample	Element	Normalized quality C [wt.%]	Atomic number C [atm.%]
12.5%-Zr-In_2O_3	In	72.85	29.99
	O	22.96	67.84
	Zr	4.18	2.17
14.5%-Zr-In_2O_3	In	74.37	31.90
	O	21.38	65.81
	Zr	4.25	2.30
16%-Zr-In_2O_3	In	69.17	26.82
	O	25.34	70.51
	Zr	5.49	2.68
20%-Zr-In_2O_3	In	67.63	25.67
	O	26.21	71.39
	Zr	6.16	2.94

Table S2 PEC water splitting performance of some In_2O_3-based photoanodes.

Photoanodes	Synthesis Method	Substrate	Light Source	Electrolyte	Photocurrent Density	Ref.
cubic In_2O_3	chemical bath reaction method	FTO	35 mW·cm^{-2}	0.1M Na_2SO_4 (pH=7)	1.15 mA·cm^{-2} at 1.51 V vs RHE	1
In_2O_3 nanorods	electrodeposition	FTO	-	1M CH_3OH, NaOH (pH=12)	2.0 μA·cm^{-2} at 0 V vs Ag/AgCl	2
In_2O_3 nanostructures	solvothermal method	FTO	100 mW·cm^{-2}	0.1M NaOH	0.4 mA·cm^{-2} at 1.30 V vs RHE	3
In_2O_3/In_2S_3 heterostructures	two-step hydrothermal method	FTO	-	1 M NaOH	0.53 mA·cm^{-2} at 1.23 V vs RHE	4
Mn-doped In_2O_3 film	RF-magnetron sputtering technique	Si	160 mW·cm^{-2}	1 M NaOH	120 μA·cm^{-2} at 0.4 V vs Ag/AgCl	5
Indium Oxide Microcubes	chemical-bath-deposited	ITO	100 mW·cm^{-2}	1M KOH	0.44 mA·cm^{-2} at 0.5 V vs Ag/AgCl	6
Sub-50 nm nanoporous In_2O_3 spheres	solvothermal	FTO	-	0.1M Na_2SO_4	1.9 mA·cm^{-2} at 0.65 V vs Ag/AgCl	7
In_2O_3 Nanowires	chemical vapor deposition (CVD)	Si	270 mW·cm^{-2}	1 M NaOH	0.21 mA·cm^{-2} at 0.22 V vs Ag/AgCl	8
Nitrogen doped In_2O_3 thin film	solvothermal	FTO	130 mW·cm^{-2}	1.0 M KOH	140 μA·cm^{-2} at 0.4 V vs Ag/AgCl	9
Zr-doped In_2O_3 film	hydrothermal method	FTO	100 mW·cm^{-2}	0.1 M NaOH	0.30 mA·cm^{-2} at 1.50 V vs RHE	This work

Table S3 The Nyquist plots fitting results of the undoped In_2O_3 and 14.5%-Zr-In_2O_3.

Sample	R_s (Ω·cm^2)	R_{ct} (Ω·cm^2)
undoped In_2O_3	31.21	4364
14.5%-Zr-In_2O_3	28.27	2885

Table S4 Flat-band potentials and donor densities originated from the linear portion of the Mott–Schottky plots that shown in Fig. 9b in the main text.

Sample	**Flat-band potential (V *vs*. RHE)**	**Donor density (cm^{-3})**
undoped In_2O_3	0.55	3. 60×10^{21}
14.5%-Zr-In_2O_3	0.49	10.88×10^{21}

References

1 D. Sariket, S. Shyamal, P. Hajra, H. Mandal, A. Bera, A. Maity, S. Kundu and C. Bhattacharya, *Materials Chemistry and Physics*, 2017, **201**, 7-17.

2 J. Gan, X. Lu, T. Zhai, Y. Zhao, S. Xie, Y. Mao, Y. Zhang, Y. Yang and Y. Tong, *Journal of Materials Chemistry*, 2011, **21**, 14685-14692.

3 C. Chen, J. Moir, N. Soheilnia, B. Mahler, L. Hoch, K. Liao, V. Hoepfner, P. O'Brien, C. Qian, L. He and G. A. Ozin, *Nanoscale*, 2015, **7**, 3683-3693.

4 H. Xu, H. Chen, S. Chen, K. Wang and X. Wang, *International Journal of Hydrogen Energy*, 2021, **46**, 32445-32454.

5 X. Sun, X. Fu, T. You, Q. Zhang, L. Xu, X. Zhou, H. Yuan and K. Liu, *Electronic Materials Letters*, 2018, **14**, 733-738.

6 M. G. Mali, H. Yoon, H. Kim, B. Joshi, S. S. Al-Deyab and S. S. Yoon, *ChemPhysChem*, 2015, **16**, 3450-3457.

7 Q. Liu, W. Zhang, R. Liu and G. Mao, *European Journal of Inorganic Chemistry*, 2015, **2015**, 845-851.

8 M. Meng, X. Wu, X. Zhu, X. Zhu and P. K. Chu, *ACS Applied Materials & Interfaces*, 2014, **6**, 4081-4088.

9 K. R. Reyes-Gil, E. A. Reyes-García and D. Raftery, *The Journal of Physical Chemistry C*, 2007, **111**, 14579-14588.